This study's object is the process that forms a strengthening microrelief on the surface of profiled folding plates made of AISI 1005 and AISI 347 steels through localized indentation using a spherical indenter made of a diamond-based composite material. The principal hypothesis of the study posits that the implementation of a controlled surface texturing process enables the formation of a stable microrelief with predefined geometric characteristics. Achieving this requires establishing the regularities of microrelief formation depending on the physical and mechanical properties of the material, the geometry of the indenter, and the parameters of the contact interaction. A physical and mechanical model of the contact interaction between the indenter and the metallic plate has been built. The results of the analytical modeling were validated through profilometric measurements and 3D visualizations, which revealed differences in the depth and nature of deformation between AISI 1005 and AISI 347. The AISI 1005 steel exhibited higher plasticity and a greater tendency toward deep deformation, whereas AISI 347 demonstrated superior stability in the relief geometry. An evaluation of surface roughness parameters (Ra, Rz, Rmax) indicated that the AISI 347 steel provides better reproducibility of the strengthening effect, with average Ra and Rz values being 2–2.5 times lower than those of AISI 1005. The correlation analysis of microrelief parameters revealed a strong relationship between Ra and Rz values, with a correlation coefficient ranging from 0.93 to 0.96. This finding confirms the stability of the microrelief formation mechanism and justifies the use of AISI 347 steel in combination with a ∅3.5 mm indenter. The results of this study can be applied for manufacturing folding elements with enhanced wear resistance and geometric stability under cyclic loading conditions

Keywords: strengthening microrelief, texturing, surface topography, diamond indenter, folding systems, profilograms

UDC 686.1.023.2
DOI: 10.15587/1729-4061.2025.331742

CONSTRUCTION OF A PHYSICAL-MECHANICAL MODEL OF REINFORCING MICRORELIEF FORMATION ON PROFILED STRIPS MADE OF AISI 1005 AND AISI 347 STEELS CONSIDERING SURFACE TOPOLOGY

Petro Kyrychok
Doctor of Technical Sciences, Professor
Director*
Dmytro Paliukh
Corresponding author
PhD Student
Department of Reprography*
E-mail: paluhdmi@gmail.com
*Educational and Scientific Institute
for Publishing and Printing
National Technical University of Ukraine
"Igor Sikorsky Kyiv Polytechnic Institute"
Beresteiskyi ave., 37, Kyiv, Ukraine, 03056

Received 04.03.2025
Received in revised form 13.05.2025
Accepted 30.05.2025
Published 27.06.2025

How to Cite: *Kyrychok, P., Paliukh, D. (2025). Construction of a physical-mechanical model of reinforcing microrelief formation on profiled strips made of AISI 1005 and AISI 347 steels considering surface topology. Eastern-European Journal of Enterprise Technologies, 3 (1 (135)), 17–29. https://doi.org/10.15587/1729-4061.2025.331742*

1. Introduction

In modern printing production, in particular in the manufacture of integral covers, the task of ensuring high bending accuracy, wear resistance, and geometric stability of profile folding strips is becoming increasingly relevant. The conditions of repeated cyclic loading during folding require these elements not only to have sufficient rigidity but also to have increased resistance to surface wear, deformation accumulation, and loss of profile accuracy.

In this context, methods of localized surface strengthening are of particular importance as they make it possible to simultaneously increase the service life of folding strips and ensure the stability of the geometry of guide zones [1].

One of the promising areas is the texturing technology, which is implemented by pressing a spherical indenter made of reinforced diamond composite heat-resistant material obtained under conditions of ultra-high pressure and temperature.

This approach allows the formation of a strengthening microrelief due to the development of zones of plastic deformation and the formation of residual compressive stresses. In the case of austenitic steel AISI 347 (American Iron and Steel Institute), this also contributes to the initiation of martensitic-type phase transformations. As a result, targeted local strengthening of the surface is achieved without the need for thermal or chemical-thermal treatment of the entire part.

For a comprehensive study of these processes, the work combines analytical modeling of the stress-strain state with experimental formation of microrelief and assessment of its geometric characteristics. Special attention is paid to the analysis of the surface topology (depth, symmetry, stability of microgrooves), which determines the nature of the contact interaction with bending elements and affects the functioning of the folding unit.

Taking into account the complex dependence of relief parameters on the properties of steel, the geometry of the indenter and the processing modes, a mathematical generalization of contact interaction models and verification of their results by 3D modeling and profilometry was carried out.

Scientifically interesting is the comparison of the effectiveness of local strengthening for steels of different nature – structural low-carbon (AISI 1005) steel and austenitic corrosion-resistant (AISI 347) steel. The study also pays special attention to the parameters of the roughness of the formed surface, the reproducibility of the micro profile, and the correlations between the characteristics of the relief.

Validation of such a model requires a coordinated analytical and experimental analysis – taking into account profilometry data, roughness parameters, depth of plastic deformation, and spatial stability of the formed microrelief. This determines the relevance of the proposed research area.

2. Literature review and problem statement

In modern research, the direction of strengthening the working surfaces of steel elements using microrelief formation methods is actively evolving. This is due to the need to increase the wear resistance, stability of geometry and resource of structural elements, in particular, folding strips in the printing industry. Attention is growing to the formation of a controlled surface topology, which determines the functional efficiency of contact elements under cyclic loading modes.

In paper [1], analysis of the formation of a strengthening microrelief under the influence of laser pulsed impact on steel strips made of AISI 1005 and AISI 347 steels was carried out. The authors emphasize the increase in hardness and wear resistance due to uniform hardening but the use of indenters for forming a local profile, which is the basis of the texturing technology proposed in this work, was not considered.

In study [2], the technology of vibration rolling was considered as a method of forming a regular microrelief on flat surfaces. Dependences are given to assess the efficiency of the process but the specificity of the curved surfaces of profile strips and the peculiarities of change in surface topology under local loading by an indenter are not taken into account.

The authors of work [3] focused on frictional electro pulse smoothing and aluminothermic hardening. It was found that these methods improve wear resistance but there is no data on micro profiling and the functional role of topologically structured relief in ensuring the durability of elements.

In [4], a systematic analysis of surface chrome plating and anodizing methods was carried out. Although a wide range of surface hardening methods is covered, local deformation or indentation methods that form the microrelief topology of the surface, relevant for folding elements, are not considered.

In [5], a method for analyzing contact problems of thin-walled elements is proposed. However, attention is focused on thermal loading and frictional heating, and not on the implementation of texturing technology and the formation of a microrelief that provides hardening.

In [6], the results of studies on the influence of a partially regular relief obtained by ball rolling on microhardness are reported. The dependence of the hardening depth on groove density and feed rate is established, but AISI 1005 and AISI 347 steels and their behavior under controlled texturing of curved elements are not taken into account.

In [7], a review of methods for strong plastic deformation of the surface is given. Despite a detailed analysis of structural changes, there is no consideration of methods aimed at creating a functionally justified surface topology.

In study [8], a numerical model for predicting surface deformation during mechanical attrition was proposed. However, the work did not consider the formation of a regular profile or the effects of residual stresses after indentation in the context of texturing technology.

In paper [9], the mechanism of indentation of a combined hardened layer under hydrogen exposure was investigated. The authors analyzed the behavior of low-alloy steel but the issue of the formation of topological microrelief was left out of consideration.

In work [10], the effect of the indentation size on the microhardness of Hadfield steel was studied. Despite its scientific value, there is no analysis of the geometric texturing of the profile surfaces of folding elements.

In paper [11], approaches to modeling the effect of indentation size in crystalline materials were considered but the applied problems of micro profile formation remained out of focus.

In study [12], a method for analyzing the rough contact of complex profile elements with an intermediate layer model was proposed. This builds a basis for building computational models but does not take into account the parameters of the surface topology after the formation of the microrelief.

Our review of the literature [1–12] reveals the active development of methods for surface strengthening of metallic materials using local plastic deformation, ball rolling, laser hardening, and methods of severe plastic deformation. Numerous works have investigated the influence of technological parameters on the microhardness, roughness, and microstructure of the near-surface layer, as well as the effects of the imprint size.

At the same time, the cited papers do not provide a comprehensive approach to the formation of a reinforcing microrelief on profile folding strips made of AISI 1005 and AISI 347 steels. These elements operate under cyclic loading conditions in printing systems.

The regularities of micro profile formation under the action of an indenter with a diamond composite tip, as well as the influence of texturing technology parameters on the surface topology, its geometric stability and wear resistance, have not been investigated.

In addition, materials of different nature, in particular low-carbon structural steel AISI 1005 and austenitic corrosion-resistant steel AISI 347, demonstrate different sensitivity to localized loading. This is manifested in differences in the mechanisms of plastic deformation, dislocation strengthening, substructural stabilization, and susceptibility to phase transformations.

Therefore, it is advisable to conduct a study aimed at constructing a generalized physical and mechanical model of the process that forms a reinforcing microrelief. Such a model should take into account the mechanical properties of the material, the geometry of the tool, the loading parameters, as well as regularities in the formation of a surface with optimal topological characteristics.

3. The aim and objectives of the study

The aim of our research is to build a generalized physical and mechanical model of the process that forms a reinforcing microrelief on the surface of profile folding strips made of

AISI 1005 and AISI 347 steels under local indentation conditions. The results to be obtained could allow us to justify the choice of material and geometry of the tool to ensure the stability of the guide elements and increase the wear resistance of folding systems.

To achieve the set goal, the following tasks are planned:

– to conduct an analysis of the physical and mechanical properties of AISI 1005 and AISI 347 steels and to build a physical and mechanical model of the contact interaction of the indenter with the materials of the plates;

– to conduct an analytical and experimental study of the microrelief, within which to determine the contact geometry, mechanical parameters, and the indentation profile, confirmed by the results of 3D modeling and profilometric measurements;

– to perform a quantitative assessment of the roughness parameters (*Ra*, *Rz*, *R*max) and an analysis of reproducibility of the microrelief after hardening, taking into account the influence of the type of steel and the diameter of the indenter;

– to carry out a correlation analysis of surface roughness parameters and, based on the resulting dependences, justify the feasibility of choosing the steel grade and indenter geometry.

4. The study materials and methods

The object of our study is the process that forms a strengthening microrelief on the surface of profile folding strips made of AISI 1005 and AISI 347 steels by local indentation of a spherical indenter made of diamond composite material.

For experimental studies, samples of plates of standard sizes 100 × 20 × 2 mm were prepared. AISI 1005 steel belongs to structural low-carbon steels and is characterized by high plasticity and the ability to intensively grind grains in the deformation zone. In contrast, AISI 347 steel is an austenitic corrosion-resistant steel, characterized by increased hardness and microstructural stability.

The basic physical and mechanical properties of AISI 1005 and AISI 347 steels, which are of priority importance for analyzing the microrelief strengthening process, are given in Table 1.

Control methods and measuring instruments (Table 2) ensure the accuracy and reliability of the process that forms guides with microrelief. For this purpose, an indenter with a spherical tip reinforced with a diamond composite heat-resistant material of increased wear resistance (AKTM+) was used. This material was obtained at the V. M. Bakul Institute of Superhard Materials, NAS of Ukraine, by sintering under ultrahigh temperatures and pressures (UHT) of diamond micro powders with the addition of multilayer graphene ($n \geq 2$) in a concentration of 0.01–0.30% by weight [12].

Microrelief hardening was carried out at a specialized bench (a fragment of the scheme of its mechanism is shown in Fig. 1), which provided:

– constant indentation force: 50, 100, and 150 N;

– controlled plate movement speed: from 0.1 to 10 mm/s;

– linear movement of the plate along a fixed indenter.

Table 1

Basic properties of AISI 1005 and AISI 347 steels

No.	Indicator	AISI 1005	AISI 347
1	Chemical composition (basic element)	Low carbon steel. Main elements: C (0.05%), Mn (0.30–0.60%), P (max 0.04%), S (max 0.05%)	Stainless steel with titanium stabilization. Main elements: C (max 0.08%), Mn (max 2.00%), Si (max 0.75%), P (max 0.045%), S (max 0.03%), Cr (17–19%), Ni (9–13%), Ti (min 10 × C to max 1.00%)
2	Yield limit, σ_y (MPa)	≈ 205 MPa	≈ 240 MPa
3	Tensile strength, σ_u (MPa)	≈ 345 MPa	≈ 515 MPa
4	Relative elongation, σ (%)	≈ 25%	≈ 40%
5	Young's modulus, E (GPa)	210 GPa	193 GPa
6	Microhardness, H (GPa)	≈ 1.6 GPa	≈ 2.0 GPa
7	Structure type	Ferrite-pearlite structure (due to low carbon content)	Austenitic structure (due to its high nickel and chromium content)
8	Phase stability	Stable at low temperatures, prone to corrosion	Stable at high temperatures, resistant to intergranular corrosion thanks to titanium

Table 2

Control methods and measuring instruments

Evaluated characteristic	Method of control	Applied hardware/software
Microrelief parameters (*Ra*, *Rz*, *R*max)	Contact profilometry	Mitutoyo Surftest SJ-410, Mitutoyo Corporation (Japan)
Microhardness of the near-surface layer	Vickers method	MicroMet 5104, HMV, 50 g, Buehler Ltd (USA)
Microstructure of the material	Optical metallography	Olympus GX51, Olympus Corporation (Japan)
Phase transformations	X-ray phase analysis	Rigaku Ultima I, Rigaku Corporation (Japan)
Reinforcement depth	Serial micro sections + microhardometry	MicroMet 5104 + grinding system, Buehler Ltd (USA)
Microrelief geometry	3D visualization	Surftest Analyzer/MountainsMap, Digital Surf (France)
Contact interaction	Analytical modeling	Hertz's models, MATLAB R2023a, (MathWorks Inc., USA), Excel
Experimental data processing	Digital processing of plots and number series	MATLAB R2023a (MathWorks Inc., USA)
Modeling and visualization software	Analytical modeling, 3D visualization, experimental data processing, correlation analysis	MATLAB R2023a (MathWorks Inc., USA)

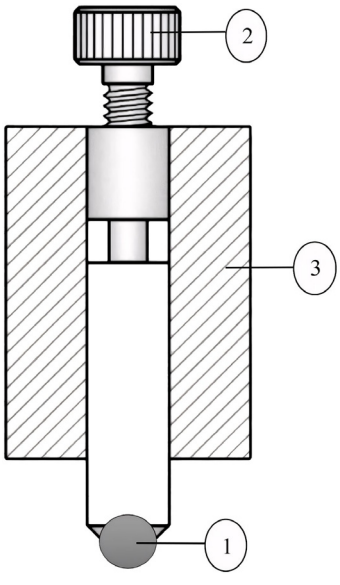

Fig. 1. Fragment of the diagram showing the indenter mechanism as part of a specialized bench: 1 — spherical carbide indenter; 2 — indenter indentation adjustment mechanism; 3 — indenter movement guides

The profiles of the guides were built in cross-section; changes in the depth of the relief were recorded at variable speeds. Hardness measurements were performed in the center of the guide every 5 μm in depth. For AISI 347, the presence of martensitic phase inclusions in the near-surface zone was additionally assessed.

The data were processed using mathematical models (exponential dependence of depth on speed and force), visualized in the form of 2D and 3D plots; maps of the distribution of strengthening in width and depth were also constructed. Additionally, a comparative assessment of the strengthening efficiency for both steels was carried out.

5. Results of investigating the formation of a reinforcing microrelief on profile folding strips

5. 1. Results of the physical and mechanical analysis of local strengthening and analytical modeling of the microrelief

On two samples of plates made of AISI 1005 and AISI 347 steels, longitudinal reinforcing microrelief guides were applied using an indenter with a tip reinforced with a diamond composite heat-resistant material of increased wear resistance (AKTM+). The geometry of the tip ensured a stable shape of the grooves, and the composite structure reduced friction and adhesion of material particles.

In the process of microrelief strengthening of plates, which is carried out by pressing the indenter with a stable programmed load while moving the plate along its surface, a set of physical and mechanical phenomena is formed (Fig. 2). These processes can be conditionally divided into several interconnected levels of contact interaction, plastic deformation, residual stresses, dislocation strengthening, and microstructural changes.

In the process of pressing a spherical indenter into a metal plate, a localized contact load occurs, concentrated in a limited contact area. As a result, a cell of concentrated stress state is formed in the near-surface zone of the plate, where hydrostatic pressure dominates, i.e., under the indenter the material experiences uniform pressure in all directions. The hydrostatic stress component can be described mathematically as the average value of normal stresses along the three coordinate axes

$$\sigma_{hyd} = \frac{\sigma_x + \sigma_y + \sigma_z}{3}, \quad (1)$$

where σ_x, σ_y, σ_z are normal stresses along the three coordinate axes.

This reduces the risk of cracks and ensures a smoother process of plastic deformation under load. Its value exceeds the yield strength of the material by ≈ 2.8 times. For AISI 1005 steel: yield strength $\sigma_\gamma \approx 205$ MPa, contact pressure – 570–590 MPa. For AISI 347 steel: yield strength $\sigma_\gamma \approx 240$ MPa, contact pressure – 650–680 MPa.

Such an excess of contact pressure ensures the loss of elastic equilibrium and initiates plastic deformation necessary for the formation of a strengthening microrelief on the surface of the folding elements. The pressure distribution in the contact zone of the hemispherical indenter is axisymmetric and decreases from the center to the periphery. It is this stress concentration that serves as a trigger for the activation of internal strengthening micro mechanisms.

After exceeding the local yield point, an intensive plastic displacement of the crystal lattices in the direction of the applied pressure occurs in the contact zone. Plastic deformation spreads from the surface deep into the material, forming a zone of intensive deformation of a hemispherical shape.

In this zone, dislocations actively evolve, and grain boundary sliding, recrystallization, and substructural processes also occur. In AISI 1005 steel, this manifests itself mainly in the form of sliding and elongation of grains, while in AISI 347 steel, it is manifested by the formation of complex dislocation structures and local work hardening zones, which provide the possibility of further strengthening.

It is important that the intensity of plastic deformation depends not only on the pressure but also on the kinematic parameters of indentation (speed of movement, time of load action) and the properties of a particular material.

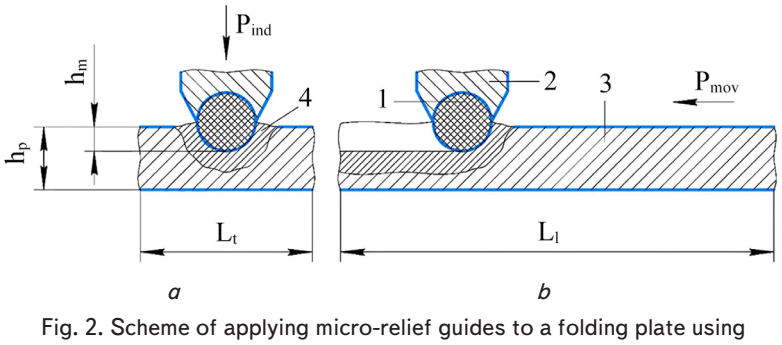

Fig. 2. Scheme of applying micro-relief guides to a folding plate using a spherical indenter: *a* — fragment of the cross-section of a micro-relief guide; *b* — fragment of the longitudinal section of a micro-relief guide; 1 — spherical indenter; 2 — fragment of the indenter holder; 3 — fragment of the folding plate; P_{ind} — indenter pressing force; P_{mov} — plate movement force; h_p — plate thickness; h_m — indentation depth; L_t — length of the fragment of the cross-section of the plate; L_l — length of the fragment of the longitudinal section of the plate

As a result of uneven plastic displacement of the material and its partial elastic recovery after the indenter is moved, a system of residual stresses is formed in the surface layers. The main role belongs to compressive residual stresses, which are formed as a result of the displacement of the metal volume and its preservation in a compacted state.

These compressive stresses are of great importance because they:

– reduce the likelihood of microcracks;

– increase fatigue strength;

– improve resistance to contact wear;

– stabilize the shape of the formed microrelief during subsequent load cycles.

In AISI 347 steel, due to the high thermal stability of the microstructure, these stresses are better preserved at elevated temperatures, which makes the material more suitable for long-term operation under difficult conditions.

During intensive plastic deformation, dislocations are actively generated in the crystal lattice of the metal – linear defects that participate in the strengthening mechanism. With increasing deformation, dislocations accumulate, interact with each other, block, and form stable configurations that prevent further sliding of atomic planes.

This leads to a local increase in hardness and resistance to plastic displacement – a classic mechanism of dislocation strengthening.

In AISI 1005 steel, which has a softer ferritic structure, dislocation strengthening is less intense but still provides an increase in microhardness in the indentation zone. In contrast, in AISI 347 steel, due to the presence of titanium carbides (TiC), which serve as effective barriers to dislocations, zones with a high degree of hardening and stable substructural stabilization are formed, which significantly increases the resource of the hardened surface.

As a result of local indentation, a deep microstructural transformation of the near-surface layer occurs, which includes:

– grain refinement due to recrystallization and the formation of subgrain boundaries;

– formation of deformation textures – oriented arrangement of crystallographic planes, which improves directional strength;

– appearance of defects such as micro twins in AISI 347 steel at high load levels;

– local disruption of phase equilibrium, especially in steels with alloying elements.

These changes create a strengthened near-surface layer, characterized by:

– increased microhardness (1.5–2 times higher than that of the base material);

– educed plasticity (which is compensated by the overall level of strength);

– higher stability of the microrelief geometry during friction and cyclic loading.

In the case of AISI 347, the microstructure remains heat-resistant, which facilitates its use under conditions of cyclic mechanical stress.

For a spherical indenter pressed into an isotropic steel plate (AISI 347 steel, AISI 1005 steel) with a force F (N), the penetration depth h (m) is related to the radius $R = D/2$ (m), and the radius of the contact zone a (m), according to the classical Hertz theory [13]

$$a = \sqrt{Rh}. \tag{2}$$

Indentation force due to contact stiffness

$$F = \frac{4}{3} E^* \sqrt{Rh^{3/2}}, \tag{3}$$

where E^* is the reduced modulus of elasticity (Pa)

$$\frac{1}{E^*} = \frac{1-\upsilon_1^2}{E_1} + \frac{1-\upsilon_2^2}{E_2}, \tag{4}$$

where E_1, E_2 – Young's moduli for the indenter (AKTM+) and steel, respectively (Pa); υ_1, υ_2 – Poisson's ratios for the indenter and steel, respectively (–).

Using the reduced modulus of elasticity E^* allows us to reduce the contact of two bodies with different mechanical properties to the equivalent interaction of a conditional homogeneous body with a generalized modulus of elasticity. This approach simplifies the calculation procedures, allowing us to apply universal analytical relations, in particular the equation of contact interaction according to Hertz's theory. In addition, it allows us to obtain an approximate, but physically justified estimate of the stiffness response of the system in the contact zone.

The plate slides along a fixed indenter. In this case, the distribution of stresses in the direction of motion x on the contact surface is considered.

Contact pressure

$$p(x) = p_0 \sqrt{1 - \left(\frac{x}{a}\right)^2}, \; |x| \le a, \tag{5}$$

where p_0 is the maximum contact pressure; a is the half-length of the contact area.

Consider a small element of the sliding path dx, then the change in plastic deformation ε_p can be described by the relation

$$d\varepsilon_p = \frac{\tau(x)}{\sigma_y} dx, \tag{6}$$

where $\tau(x)$ – tangential stress at the slip limit; σ_y – yield strength of steel.

This allows us to model the accumulation of plastic deformation along the direction of movement and to estimate the relief profile after the indenter passes.

The final differential expression describing the change in the depth of the formed microrelief along the direction of movement of the indenter takes the following form

$$\frac{dz(x)}{dx} = \phi \cdot \frac{p(x)}{\sigma_y}, \tag{7}$$

where $p(x)$ is the normal (contact) pressure acting on the plate; ϕ is the empirical coefficient of relief formation, depending on the stiffness of the plate and the properties of ACTM+; $z(x)$ is the profile of the relief deepening.

Formula (7) describes the geometric profile of the microrelief formed as a result of the action of contact pressure. When the plate moves along a spherical indenter with a constant indentation force, the profile of the microrelief and the degree of strengthening are determined by the sliding speed. The dependence is described as follows:

– the time of contact of the material with the indenter

$$t_c = \frac{2R}{v}, \tag{8}$$

where t_c is the local contact time; R is the radius of the spherical indenter; v is the plate movement speed;

– plastic deformation energy per unit volume

$$w_p = \sigma_y \cdot \varepsilon_p\left(t_c\right), \tag{9}$$

where ε_p is the plastic deformation that depends on the contact time;

– dependence of relief depth on speed

$$h_v = h_0 \cdot \exp\left(-k \cdot v\right), \tag{10}$$

where h_0 is the maximum depth at slow displacement ($v \to 0$); k is an empirical coefficient that takes into account the sensitivity of the material to the deformation rate.

Depending on the properties of the steel, the nature of the influence of the displacement rate on the depth of the relief differs significantly: for AISI 1005 steel, which is characterized by high plasticity [14] $k_v^{1005} < k_v^{347} \to$ the depth decrease occurs more slowly, which indicates its ability to maintain the shape of the relief even at increased deformation rates.

In contrast, for AISI 347 steel, which has higher hardness [15], not only a more intense depth decrease with increasing velocity v is observed, but also a noticeable decrease in the intensity of deformation-induced phase transformations.

This limits the degree of local strengthening under high-speed contact conditions.

Within the framework of modeling the contact interaction of a spherical indenter with the plate surface, the distribution of tangential and normal stresses that arise in the local contact zone during sliding is considered. In this context, that is, within the analytical model of strain accumulation (equation (6)) and geometric formation of the relief (equation (7)), tangential stresses acting on the contact boundary cause local plastic deformation of the material.

This deformation, gradually accumulating along the indenter sliding trajectory, leads to the formation of a depression on the surface. Since the nature of this depression is determined by the change in local plastic deformation along the direction of movement, its geometric description is implemented through the function of the relief depth change $z(x)$, given in formula (7). Thus, the mathematical description of the relief profile is based on the physical connection between the tangential stress field and the result of their action – the formation of a depression on the surface of the plate.

Both mathematical expressions are components of a single physical model of contact interaction, where there is a direct connection between the stress field and the geometric parameters of the formed relief (Fig. 3).

Based on our physical and mechanical analysis, it was established that the process of local strengthening of profile steel plates by pressing a spherical indenter is accompanied by a number of interrelated phenomena. Among them are the development of zones of plastic deformation, the formation of residual compressive stresses, dislocation strengthening, and microstructural changes in the surface layer. A model of contact interaction between the indenter and the material has been built, which combines the equations of contact pressure and the indentation profile.

This model allows us to describe the regularities of the formation of the strengthening microrelief as a function of the mechanical properties of the material, kinematic parameters, and geometry of the tool. The geometry of the tool in this model is taken into account through the empirical coefficient of relief formation ϕ, which is included in equation (7) and depends on the radius of curvature of the hemispherical indenter, the rigidity of the plate, and the characteristics of the contact pair.

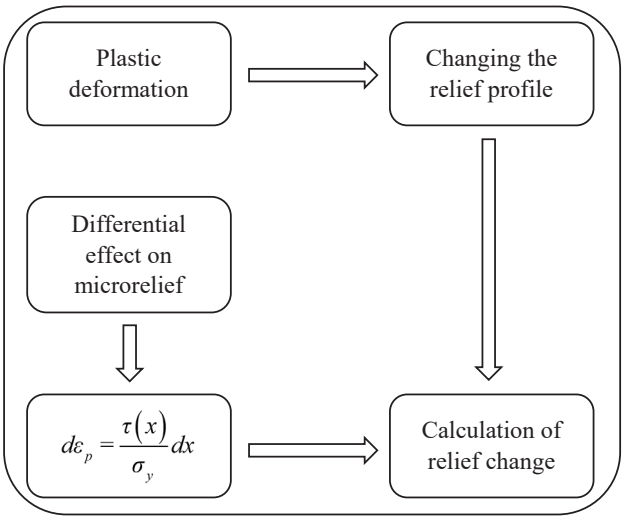

Fig. 3. Visualization of the relationship between plastic deformation and microrelief profile formation

5. 2. Results of analytical modeling and experimental-model analysis of microrelief geometry during local strengthening

The results of analytical modeling and experimental analysis of microrelief geometry during local strengthening include both numerical reconstruction of the profile in the MATLAB environment and processing of real profilometric measurements obtained from samples after indentation. This approach allows us to compare model predictions with the physical morphology of the formed surface.

Based on the formed physical-mathematical model of the relationship between the stress-strain state of the material and the geometry of the surface microrelief, it is advisable to perform a quantitative assessment of the main parameters of contact interaction for specific engineering materials. This allows us to verify the applied effectiveness of the proposed model and deepen our understanding of the role of physical-mechanical characteristics in the process of forming a strengthening relief.

Taking into account the physical interpretation of formulas (2) and (3), their practical application is considered. In order to quantitatively assess the influence of the mechanical properties of the material on the parameters of contact deformation, analytical modeling was performed based on generalized physical and mechanical dependencies. Taking into account formulas (2) to (5), a quantitative assessment of the parameters of contact interaction for specific materials was carried out. Based on the specified mechanical characteristics of AISI 347 and AISI 1005 steels, the main parameters of contact interaction were calculated. These parameters include the half-width of the contact zone, the value of the maximum contact pressure, and the reduced modulus of elasticity, which determine the geometry of the formed relief.

To ensure the objectivity of the comparative analysis, all calculations were performed under the same initial conditions. This allows for a reasonable assessment of the influence of the physical and mechanical characteristics of the material on the parameters of contact interaction when forming microrelief guides on the working surface of folding strips.

Taking into account the geometric characteristics of the indenter, as well as the elastic moduli and Poisson's ratios of

both the indenter and the steel samples AISI 347 and AISI 1005, the initial physical and mechanical parameters of the contact interaction were determined. Based on these data, calculations were performed of the reduced elastic modulus of the contact system, the half-width of the contact spot, the indentation force, and the maximum contact pressure. The calculations were carried out using formulas (2) to (5), which take into account the geometry of the contact and the nonlinear nature of the load when pressing the body of rotation into a flat surface. Such calculation parameters enable a quantitative assessment of the intensity of the local load and the nature of the formation of the stress-strain state in the contact zone. The summarized initial data and calculation results for both types of steel are given in Table 3.

Together with the results obtained from the calculations, the generalized data are given in Table 4. This makes it possible to carry out a comparative analysis of the influence of material properties on the formation of microrelief, in particular, it is possible to trace the dependence of the geometric parameters of the contact zone on the modulus of elasticity, yield strength, and Poisson's ratio of the studied steels.

Our results constitute a methodological basis for further analysis of the features of elastic and plastic deformation of contacting bodies. They also serve as a methodological basis for specifying the criteria for rational selection of materials in the tasks of microstructural shaping of microrelief guides on the working surface of profile folding strips.

To visualize the influence of the mechanical properties of the material on the parameters of relief formation, below are diagrams of the dependence between the maximum contact pressure and the corresponding depth of microrelief guides, formed using the MATLAB software (Fig. 4,). This approach allows us to track the change in the geometry of the recess depending on the resistance of the material to plastic deformation, which is of great importance for further engineering interpretation of the results. To illustrate the features of the formation of microrelief in the contact zone of the indenter with steel plates, two types of graphical representation were used: a 3D model and a 2D heat map. Both images are supplemented with a color scale of deformation depth (Fig. 4, 5).

The 3D models (left) depict a three-dimensional model of the relief formed by the indentation of a spherical indenter. The color scale accompanying both 3D models serves to conditionally encode the depth of the relief: dark colors (blue, purple, red) correspond to the maximum depth, and light shades (yellow, pink, light green) correspond to elevated areas of the surface.

Table 3

Summary of input data and calculation results

Indicator	AISI 347	AISI 1005
Indenter diameter, mm	2.5	2.5
Indenter radius R, mm	1.25	1.25
Indentation depth h, mm	0.75	0.75
Young's modulus of the indenter E_1, MPa	800000.0	800000.0
Poisson's ratio of the indenter ν_1	0.1	0.1
Young's modulus of the plate E_2, MPa	190000.0	210000.0
Poisson's ratio of the plate ν_2	0.3	0.29
Reduced modulus of elasticity E^*, MPa	165920.75	178605.6
Half-width of the contact patch a, mm	0.9682	0.9682
Indentation force F, N	160652.08	172934.13
Maximum contact pressure p_0, MPa	81819.43	88074.63

Table 4

Comparative analysis of the influence of material properties on the formation of microrelief on the working surface of folding plates

Material	Indenter D (mm)	h (mm)	E^* (MPa)	a (mm)	F (N)	p_0 (MPa)
AISI 347	2.5	0.5	165920.75	0.7906	87447.91	66805.29
AISI 1005	2.5	0.5	178605.6	0.7906	94133.42	71912.63
AISI 347	2.5	0.75	165920.75	0.9682	160652.08	81819.43
AISI 1005	2.5	0.75	178605.6	0.9682	172934.13	88074.63
AISI 347	2.5	1.0	165920.75	1.118	247340.05	94476.94
AISI 1005	2.5	1.0	178605.6	1.118	266249.51	101699.82
AISI 347	3.5	0.5	165920.75	0.9354	103469.77	56460.77
AISI 1005	3.5	0.5	178605.6	0.9354	111380.16	60777.27
AISI 347	3.5	0.75	165920.75	1.1456	190086.1	69150.04
AISI 1005	3.5	0.75	178605.6	1.1456	204618.42	74436.65
AISI 347	3.5	1.0	165920.75	1.3229	292656.7	79847.59
AISI 1005	3.5	1.0	178605.6	1.3229	315030.67	85952.04

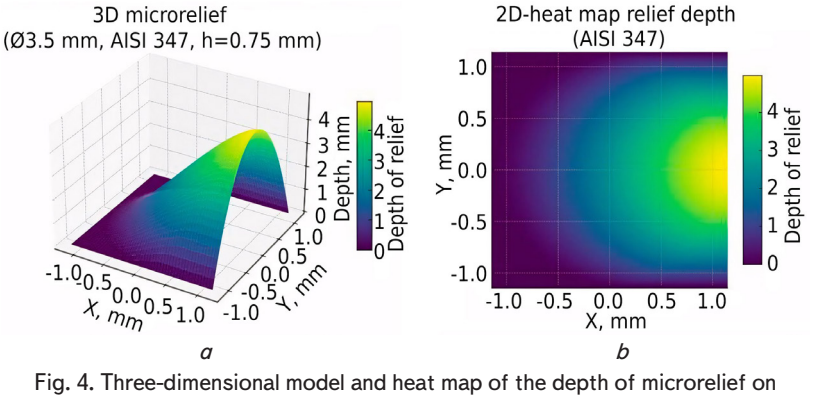

a *b*

Fig. 4. Three-dimensional model and heat map of the depth of microrelief on the surface of an AISI 347 stainless steel plate: *a* — three-dimensional model of microrelief, *b* — two-dimensional heat map of the distribution of the depth of relief

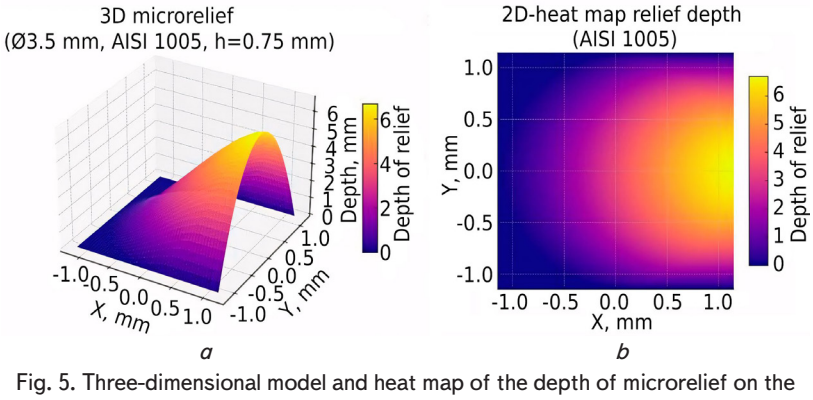

a *b*

Fig. 5. Three-dimensional model and heat map of the depth of microrelief on the surface of a plate made of AISI 1005 carbon steel: *a* — three-dimensional model of microrelief, *b* — two-dimensional heat map of the distribution of the depth of relief

For a detailed analysis of the relief topography, 2D depth color distribution maps (right) are also provided. These maps display the same depth distribution, but in the form of a flat color map, where each point has a corresponding color value for depth.

This representation facilitates the study of radial symmetry, contact patch area, and localization of zones of maximum influence.

The results of visualization in the form of three-dimensional relief models and corresponding heat maps obtained after indentation of spherical indenters provide a qualitative idea of the nature of plastic deformation of the material in the zone of local loading.

They make it possible not only to assess the geometry of the contact trace but also track the differences in the behavior of steels of different types under the same loading conditions. To assess the nature of the formed microrelief and clarify the geometric features of the deformation of the material in the contact zone, detailed removal of transverse surface profilograms was performed (Fig. 6, 7).

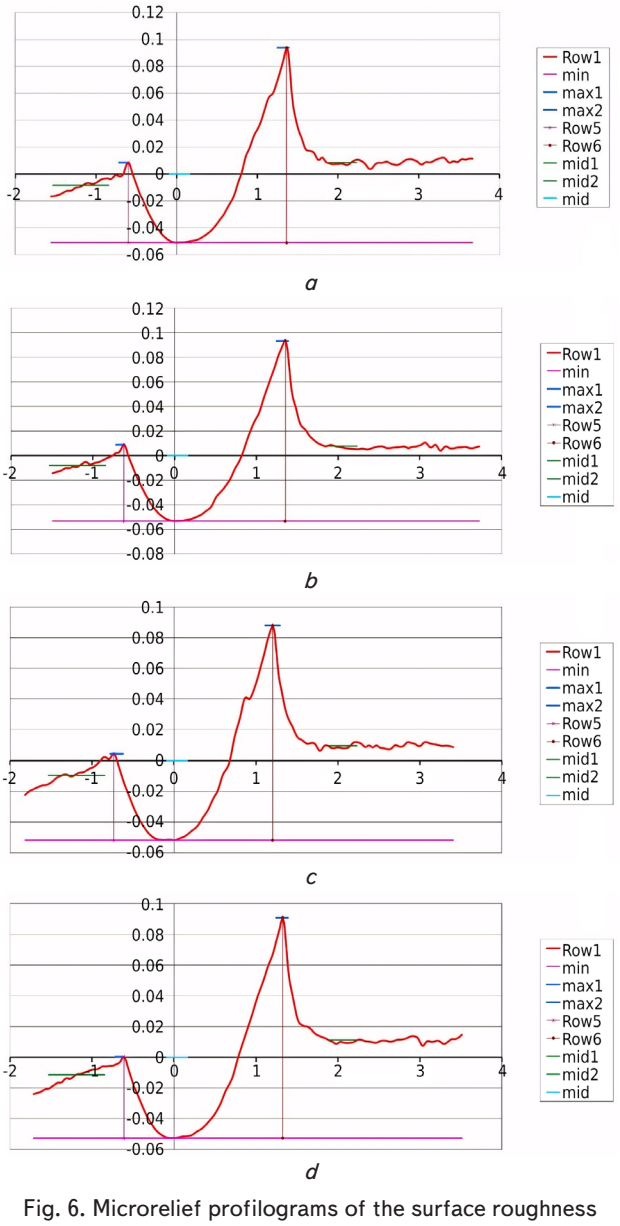

Fig. 6. Microrelief profilograms of the surface roughness of a plate made of AISI 1005 steel after hardening with a spherical indenter: *a*, *b*, *c*, *d* — samples ST1—ST4 (Table 5)

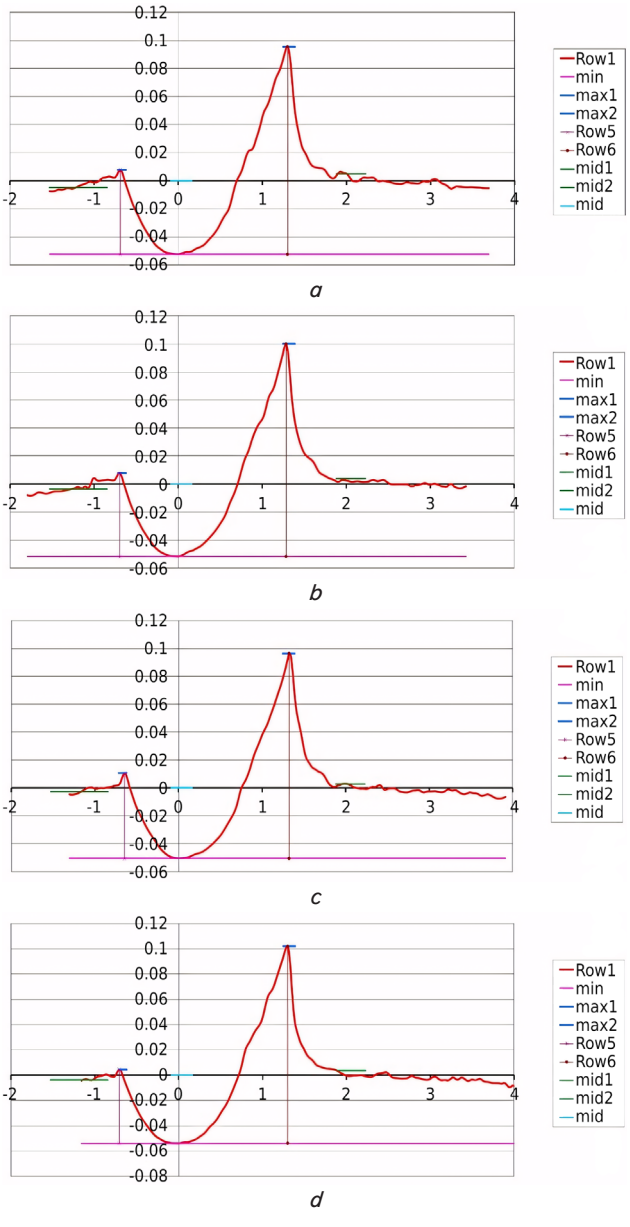

Fig. 7. Microrelief profilograms of the surface roughness of a plate made of AISI 347 steel after hardening with a spherical indenter: *a*, *b*, *c*, *d* — samples H1, H3, H5, H8 (Table 6)

Fig. 6, 7 show profilograms obtained as a result of measuring the surface micro profile in the local strengthening zone using indentation. The red curve (Row1) displays the main primary profile, constructed according to the height coordinates in the direction of the measurement trajectory.

The plot shows key points and auxiliary curves:

– min – the lowest point of the profile (maximum depth of the depression), which arose as a result of indentation;

– max1 and max2 – maximum peak values on both sides of the indentation center, indicating deformational displacement of the material;

– mid1 and mid2 – local averaged values of the profile from the left and right sides relative to the central axis;

– mid – global average value along the entire length of the profile (analogous to the overall Ra), shown by a purple horizontal line;

– Row5 – filtered profile after digital processing, used for roughness analysis or smoothed trends;

– Row6 – residual or derivative profile formed based on the removal of the background component or baseline irregularities.

The profilograms demonstrate an asymmetric distribution of microrelief, characteristic of the process of surface strengthening by local indentation with a spherical indenter. A clearly formed depression in the center and a rise of the material on both sides are observed, which confirms the effectiveness of the formation of the strengthening microrelief.

Measurements were performed along the line of action of the indenter on the areas of the working surface after local plastic deformation.

Our profilometric study has made it possible to trace the nature of changes in the surface height of plates made of AISI 1005 and AISI 347 steels after localized exposure to a hard alloy spherical indenter. All the studied samples revealed a characteristic form of plastic deformation with the formation of a deep central depression and a pronounced peripheral peak.

It was established that samples made of AISI 1005 steel are characterized by the formation of a wider deformation zone with a smooth transition from the minimum to the maximum value of the profile height. This indicates the high plasticity of carbon steel and its tendency to deeper extrusion of the material upon contact with the indenter.

In the case of AISI 347 steel, a narrower and more concentrated profile with less pronounced extreme values was recorded, which indicates increased hardness and resistance to plastic deformation. The geometry of the microrelief after hardening is characterized by greater stability and symmetry.

5. 3. Results of analyzing the surface roughness and repeatability of microrelief after hardening by an indenter

The difference in the behavior of the microrelief of the two materials confirms the feasibility of using AISI 347 steel for elements where the stability and reproducibility of the guide surface of profile folding strips are important.

However, for a full comparison of the effectiveness of hardening profile folding strips, given the change in the microgeometry of the working surface, it is necessary to involve quantitative roughness indicators.

For this purpose, a series of laboratory measurements of surface roughness after hardening of samples made of AISI 1005 and AISI 347 steel were carried out. The roughness parameters were determined by three main criteria: the arithmetic average profile height (*Ra*), the height of irregularities at ten points (*Rz*), and the maximum profile height (*R*max).

Three independent measurements were performed for each sample, based on which the average values of the corresponding parameters were calculated. The summarized measurement results are given in Table 5 for samples made of carbon steel AISI 1005 and in Table 6 for samples made of stainless steel AISI 347.

Surface hardening with carbide indenters led to a significant reduction in roughness parameters for both AISI 1005 carbon steel and AISI 347 stainless steel.

At the same time, AISI 347 steel demonstrated significantly lower final roughness values: *Ra* – 0.12 μm versus 0.31 μm (2.5 times less), *Rz* – 0.92 μm versus 1.80 μm (2 times less), *R*max – 1.53 μm versus 3.18 μm (more than half less) – compared to the corresponding values for AISI 1005 steel.

Therefore, our results indicate a higher efficiency of the hardening process for AISI 347 steel, which ensures the formation of a smoother and more stable microrelief. The roughness parameters after processing of AISI 347 steel have lower variability between different samples (coefficient of variation ~ 18–22%) compared to AISI 1005 steel (~ 26–40%). This means that the quality of the formed microrelief on AISI 347 steel is more stable.

Table 5

Experimental measurement results for AISI 1005 carbon steel samples

Sample	St_1	St_2	St_3	St_4	St_5
Ra_1	0.502	0.160	0.187	0.249	0.273
Ra_2	0.293	0.154	0.316	0.318	0.541
Ra_3	0.311	0.249	0.279	0.486	0.320
Ra mid	0.369	0.188	0.261	0.351	0.378
Rz_1	2.950	0.960	0.950	1.970	1.410
Rz_2	1.470	0.940	1.510	1.900	3.580
Rz_3	1.700	1.680	1.380	2.810	1.800
Rz mid	2.040	1.193	1.280	2.227	2.263
$Rmax_1$	2.700	1.910	2.130	2.290	4.220
$Rmax_2$	1.690	1.070	2.190	4.390	7.400
$Rmax_3$	2.470	4.850	2.260	4.140	3.920
*R*max mid	2.287	2.610	2.193	3.607	5.180

Table 6

Experimental measurement results for AISI 347 stainless steel samples

Sample	H_1	H_2	H_3	H_4	H_5	H_6	H_7	H_8
Ra_1	0.115	0.297	0.111	0.091	0.115	0.142	0.106	0.115
Ra_2	0.100	0.121	0.131	0.104	0.098	0.139	0.130	0.099
Ra_3	0.143	0.104	0.108	0.115	0.159	0.119	0.145	0.094
Ra mid	0.119	0.174	0.117	0.103	0.124	0.133	0.127	0.103
Rz_1	0.790	1.720	0.730	0.650	0.890	0.740	0.790	0.810
Rz_2	0.720	1.600	0.940	0.670	0.680	1.040	1.000	0.740
Rz_3	1.240	0.750	0.790	0.760	1.450	0.940	1.030	0.630
Rz mid	0.917	1.357	0.820	0.693	1.007	0.907	0.940	0.727
$Rmax_1$	1.250	2.000	0.990	0.920	1.380	0.920	1.250	1.720
$Rmax_2$	1.260	2.170	1.250	1.020	0.800	1.440	1.950	1.860
$Rmax_3$	1.730	1.820	1.410	1.070	3.380	1.720	1.750	1.570
*R*max mid	1.413	1.997	1.217	1.003	1.853	1.360	1.650	1.717

In AISI 1005 steel, individual cases of anomalously high peaks (*R*max) were observed, which worsened the surface uniformity. Considering the repeatability of the hardening results, AISI 347 steel also outperforms AISI 1005 steel.

The higher hardening efficiency of AISI 347 steel is associated with both the material properties (higher hardness, ability to harden uniformly) and the optimal selection of the tool.

Analysis of the results of roughness parameter measurements revealed that a larger diameter indenter (3.5 mm) is more appropriate for forming microrelief on the surface of profiled folding strips. It provides lower average roughness values (*Ra*, *Rz*, *R*max) and lower variability of results between samples, especially for AISI 347 steel. The use of a smaller diameter indenter (2.5 mm) leads to an increase in average roughness values and an increase in the scatter of results, which is especially noticeable on samples made of softer carbon steel AISI 1005. This indicates a lower stability of the microrelief when using an indenter with a smaller diameter.

5. 4. Results of correlation analysis regarding the surface roughness and justification of material selection for folding strips

In order to establish the nature of the relationships between the main parameters of the roughness of the microrelief

of the surface of the plates, a mathematical analysis of experimental data was carried out based on Pearson's pairwise correlation coefficients [16]. The indicators were designated as $Ra_1 - Ra_3$, $Rz_1 - Rz_3$ and $Rmax_1 - Rmax_3$.

Mathematically, the Pearson's pairwise correlation coefficient for samples $X = \{x_1, x_2, ..., x_n\}$ and $Y = \{y_1, y_2, ..., y_n\}$ was calculated using the following formula

$$r_{XY} = \frac{\sum_{i=1}^{n}(x_i - \bar{x})(y_i - \bar{y})}{\sqrt{\sum_{i=1}^{n}(x_i - \bar{x})^2} \cdot \sqrt{\sum_{i=1}^{n}(y_i - \bar{y})^2}}, \quad (11)$$

where x_i, y_i are the individual values of samples X and Y; $\bar{x}, \bar{y}$ – average values of corresponding samples; n – number of observations in the sample.

Using the MATLAB program, a correlation matrix of roughness parameters was constructed (Fig. 8) to detect the presence of linear dependences between individual pairs of parameters.

To make it easier to perceive the values of the Pearson correlation coefficients among the microrelief roughness parameters, color coding of the correlation matrix cells was used (Table 6).

Each value of the correlation between two variables is indicated by color according to the scale corresponding to its numerical value within the scale from –1 to +1.

The most pronounced positive correlations are observed between the values of *Ra* and *Rz* for each measurement, in particular: $Ra_1 - Rz_1 = 0.96$, $Ra_2 - Rz_2 = 0.93$, $Ra_3 - Rz_3 = 0.96$. This indicates the stability and consistency of the formation of the overall surface roughness and the characteristic height of micro-roughness.

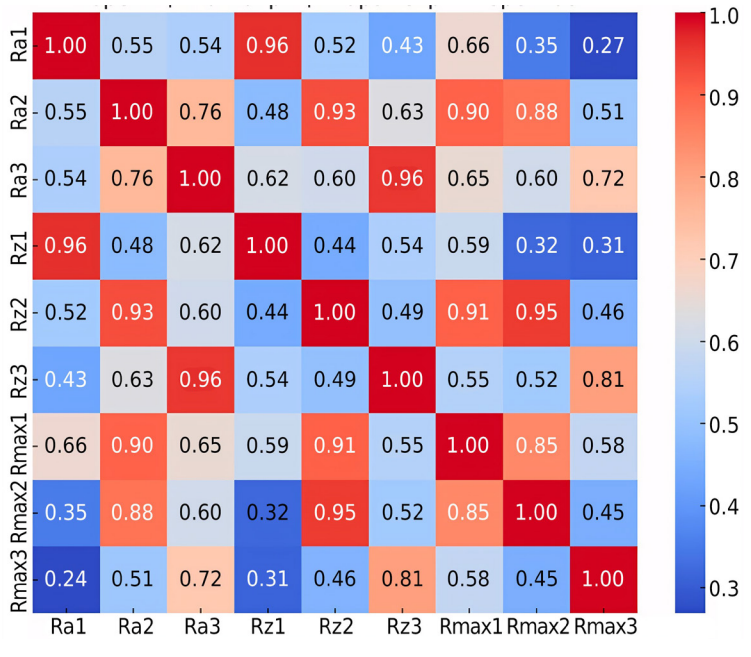

Fig. 8. Correlation matrix of roughness parameters

Table 6

Color coding of correlation matrix cells

Correlation coefficient (r)	Relation interpretation	Color coding
from +0.90 to +1.00	High degree of direct correlation	Deep red
from +0.70 to +0.89	Stable positive correlation	Light red/pink
from +0.50 to +0.69	Moderate direct correlation	Light orange
from +0.30 to +0.49	Positive low power correlation	Light yellow

High values of the correlation coefficients were also found between the parameters *Rz* and *Rmax*, which confirms the close relationship between the average profile depth and the largest local deviations. In particular, for the second measurement, the correlation $Rz_2 - Rmax_2 = 0.95$ was established, which indicates a regularity in the roughness profile.

At the same time, weaker relationships were also found in the correlation matrix, for example, between Ra_1 and $Rmax_3$ (0.27) or Rz_1 and $Rmax_3$ (0.31). These relationships may indicate local variability of microrelief, caused both by the heterogeneity of the material structure and by the peculiarities of the indentation process in different areas.

The correlation coefficients are arranged in the form of a symmetric matrix covering all pairs of *Ra*, *Rz*, and *Rmax* for three series of measurements. The obtained values exceeding 0.9 indicate the presence of a strong direct correlation and confirm the stability of the formation of microrelief during the hardening process. Values below 0.4 indicate probable profile fluctuations or differences in the structure of the surface layer.

In general, the results of the correlation analysis confirm the high consistency among the main roughness parameters within individual zones of influence of the indenter, which confirms the stability and controllability of the microrelief hardening process.

In the context of practical use for profile strips for folding strips of integral covers, it is more expedient to use AISI 347 stainless steel with additional processing with a ∅3.5 mm indenter. This will ensure minimal surface roughness and stable relief, which will contribute to higher wear resistance, tightness, and durability of the unit. Carbon steel AISI 1005, despite its lower cost and ability to more easily undergo plastic deformation, after hardening is characterized by higher values of surface roughness and less homogeneity of microrelief.

The use of AISI 1005 steel is advisable mainly in structurally less loaded or secondary elements, where the requirements for the stability of the guide profile are less significant than in folding systems of integral covers. In general, the results of our studies confirm the functional advantages of AISI 347 stainless steel in ensuring the formation of high-quality and stable microrelief of the guide surfaces of profile folding strips.

6. Discussion of results based on investigating the formation of a reinforcing microrelief on profile folding strips

The task of forming a reinforcing microrelief on the surface of profile folding strips with stable geometric characteristics under cyclic loading conditions remains relevant due to the limited effectiveness of existing methods. The approach proposed in our study allows for a stable surface morphology without structural degradation, which is a significant advantage for long-term operation.

Unlike laser hardening technologies [1, 3], in which the microrelief is formed as a result of thermal action with subsequent phase transformations, uneven cooling and loss of plasticity, the proposed approach employs a different principle. It is based on local plastic deformation of the

surface of AISI 1005 and AISI 347 steel plates using a spherical indenter (Fig. 1) made of reinforced diamond composite material (AKTM+). This approach makes it possible to form a reinforcing relief without heating, which helps preserve the microstructural stability of the surface layer.

During the indentation with a constant load, complex physical and mechanical phenomena are formed during the movement of the plate along its surface (Fig. 2). The contact pressure is distributed axisymmetrically, exceeding the yield strength of the material by approximately 2.8 times, which activates micro mechanisms of dislocation strengthening without structural degradation [6, 7]. As a result, a zone of intense deformation of a hemispherical shape is formed, within which a strengthened near-surface layer with a microhardness that is 1.5–2 times higher than the value for the base material appears.

In this zone, dislocation processes, grain boundary sliding, as well as recrystallization and substructural changes evolve. For AISI 1005 steel, sliding and grain elongation mechanisms prevail, which indicates its high plasticity. In AISI 347 steel, the formation of complex dislocation structures and local work hardening zones is observed, which determines its higher ability to harden.

To quantitatively explain the identified microstructural effects, a physical-mechanical model of contact interaction was built, based on modified provisions of Hertz theory [13]. The model makes it possible to estimate the depth of the deformation zone, the contact area, the half-width of the loaded region and the reduced modulus of elasticity taking into account the indenter geometry and the physical-mechanical properties of steels. This provides high reliability in predicting the structure of the hardened layer and the possibility of engineering optimization of the hardening parameters.

The use of the reduced modulus of elasticity E^* in the modeling of contact interaction allowed us to reduce the problem to an equivalent system of a conditionally homogeneous material with generalized characteristics. This significantly simplified the analytical evaluation procedure and provided the possibility of using universal equations (5) to (7) to calculate the basic parameters of contact interaction.

Based on the initial data (Table 3), the reduced modulus of elasticity of the contact system, the half-width of the contact spot, the indentation force, and the maximum contact pressure were calculated. The calculation of the contact interaction parameters for AISI 1005 and AISI 347 steels was carried out using formulas (2) to (5), which take into account the geometry of the indenter and the nonlinear nature of the load during the indentation of the body of rotation into a flat surface. The results summarized in Table 4 allowed us to conduct a comparative analysis of the influence of the physical and mechanical properties of materials on the nature of the formation of microrelief.

For spatial analysis of local zones of influence, three-dimensional surface models and corresponding 2D heat maps were additionally used (Fig. 4, 5). The obtained visualizations make it possible not only to estimate the geometric parameters of the deepening, but also to identify differences in the nature of plastic deformation for different steel grades under the same loading conditions. This approach allows us to reasonably adjust the technological parameters in accordance with the properties of a particular material.

Analysis of transverse profile plots (Fig. 6, 7) confirmed the asymmetric nature of the microrelief with the formation of a central depression and peripheral elevations. In samples made of AISI 1005 steel, the deformation zone is wider with a smooth height difference, which indicates its high plasticity. In contrast, in AISI 347 steel, the relief is localized with a smaller amplitude, which indicates greater hardness and stability of the deformation response.

The roughness indicators after local strengthening are summarized in Table 5 (AISI 1005) and Table 6 (AISI 347). Our data indicate that AISI 347 provides less variability of roughness parameters and higher stability of surface quality, which is an advantage for use in elements of folding systems with increased requirements for wear resistance and accuracy of shaping.

For an in-depth analysis of the influence of the structural characteristics of the material on the stability of the surface roughness, mathematical processing of the experimental data was carried out. Using the MATLAB software environment, a correlation matrix was constructed among the main parameters of microgeometry (Fig. 8), which allowed us to identify the presence of statistically significant linear relationships among *Ra*, *Rz*, and *R*max.

The results of comparing the roughness values for samples made of AISI 1005 and AISI 347 steels after local indentation showed that all parameters for AISI 347 ($Ra = 0.12\ \mu$m, $Rz = 0.92\ \mu$m, $R\text{max} = 1.53\ \mu$m) are 2–2.5 times lower than the corresponding values for AISI 1005. In addition, AISI 347 steel demonstrates higher repeatability of the results: the coefficient of variation is 18–22%, which is almost half that of AISI 1005 (26–40%).

It was found that samples from AISI 1005 are characterized by the presence of single anomalous peaks, which reduce the uniformity of the hardened layer. This indicates a lower structural stability of the material and increased sensitivity to microheterogeneities. On the contrary, AISI 347 demonstrated the ability to form a predictable and uniform microrelief. This behavior is due to the higher hardness of the steel, resistance to local plastic deformation, and precise selection of technological parameters (load, indenter geometry, speed of movement).

Additionally, it was found that the structural stability of the microrelief in AISI 347 steel is associated with the formation of the martensite phase and the development of dislocation structures [4, 9]. This is confirmed by the high level of correlation between *Ra* and *Rz* ($r = 0.93$–0.96), which indicates a consistent mechanism of relief formation.

Analysis of the influence of tool geometry revealed that the ∅3.5 mm indenter provides a more uniform contact pressure field and reduces local stresses in the deformation zone, compared to ∅2.5 mm. This contributes to a more stable course of the hardening process regardless of the steel grade [10, 12].

The results of our study allow us to address the following problematic issues:

– to eliminate the risks of phase and thermostructural defects inherent in laser hardening [1, 3];

– to move from empirical to mathematically based design of the microrelief formation process using the local indentation method [2, 5, 11];

– to ensure high stability of microgeometry by taking into account the properties of the material and the geometry of the tool [6, 9, 10, 12].

The proposed approach creates the basis for the implementation of a low-cost, technologically simple, and reproducible procedure for local strengthening of elements of folding systems with predicted properties.

However, the study has a number of limitations that determine the directions of further work. In particular:

– profilometric analysis was carried out only in the transverse direction, without taking into account possible anisotropic effects of microstructural changes in the longitudinal plane;

– the study is limited to two steel grades (AISI 1005, AISI 347) and two variants of indenter geometry (∅2.5 mm, ∅3.5 mm); therefore, generalization of the results to other materials or tool configurations requires further experimental verification;

– the process of relief formation was considered under static loading conditions, while in operation the folding elements are subjected to cyclic mechanical effects;

– temperature factors that can change the tribotechnical properties of the surface layer were not taken into account.

The shortcomings of our study include the lack of a comprehensive analysis of the long-term effect of wear and experimental comparison with alternative methods of microrelief formation, in particular laser or ultrasonic strengthening.

Given the above, promising areas of further research are:

– three-dimensional analysis of microrelief with spatial reconstruction of topography;

– expansion of the range of materials and geometric parameters of tools;

– modeling and verification of processes under cyclic loading conditions;

– consideration of the influence of temperature factors;

– comparison of the effectiveness of mechanical strengthening with alternative methods (laser, ultrasonic, electromechanical).

The implementation of these areas could allow for a deeper understanding of the patterns of microrelief formation, ensure its long-term stability under actual operating conditions, and improve the efficiency of folding systems operating under intensive modes with high requirements for wear resistance.

7. Conclusions

1. Based on the results of our physical and mechanical analysis of local strengthening and analytical modeling of the microrelief, taking into account the properties of AISI 1005 and AISI 347 steels, it was established that local indentation is accompanied by an axisymmetric distribution of contact pressure, which exceeds the yield strength of the material by ≈ 2.8 times, causing the formation of zones of plastic deformation and residual compressive stresses. Analytical relationships among the depth of indentation, contact pressure, and dimensions of the contact zone were obtained.

2. Analytical and experimental modeling of the geometry of the microrelief for AISI 1005 and AISI 347 steels has been carried out, taking into account different indenter diameters. 3D visualization and profilogram data showed that AISI 1005 steel forms a wider and less symmetrical relief profile with deeper depressions. In contrast, AISI 347 steel provides more uniform, shallower, and technologically stable guides. The use of a ∅3.5 mm indenter allowed us to reduce the depth and spread of micro profile values, especially for carbon steel.

3. According to the results of our analysis of the roughness parameters (*Ra*, *Rz*, *R*max), a higher reproducibility of hardening was found for AISI 347 steel. The average values of *Ra* and *Rz* for this steel are 2–2.5 times lower than for AISI 1005 steel, and the variation between samples is half as much. This indicates increased structural stability of the surface layer after local deformation. The use of a ∅3.5 mm indenter additionally reduces the spread of roughness parameters.

4. Correlation analysis of the relief parameters allowed us to justify the choice of steel and indenter geometry for practical use in folding systems. A close relationship was established between the parameters *Ra* and *Rz* (correlation coefficient 0.93–0.96), which indicates the constancy of the relief formation mechanism. AISI 347 steel in combination with a ∅3.5 mm indenter is the optimal technical solution for the manufacture of critical folding elements characterized by high requirements for wear resistance and geometric stability. AISI 1005 steel is recommended for use in parts with lower operational loads.

Conflicts of interest

The authors declare that they have no conflicts of interest in relation to the current study, including financial, personal, authorship, or any other, that could affect the study, as well as the results reported in this paper.

Funding

The study was conducted without financial support.

Data availability

All data are available, either in numerical or graphical form, in the main text of the manuscript.

Use of artificial intelligence

The authors used artificial intelligence technologies within acceptable limits to provide their own verified data, which is described in the research methodology section.

References

1. Kyrychok, P., Paliukh, D. (2024). Determining of the effect of reinforcing microrelief guides on the efficiency of folding integrated covers. Eastern-European Journal of Enterprise Technologies, 4 (1 (130)), 97–111. LOCKSS. https://doi.org/10.15587/1729-4061.2024.309481
2. Dzyura, V., Maruschak, P., Semehen, V., Holovko, V., Fediv, V. (2023). Justification of the Parameters of Regular Microreliefs Formed on Flat Surfaces. Central Ukrainian Scientific Bulletin. Technical Sciences, 1 (8 (39)), 37–47. https://doi.org/10.32515/2664-262x.2023.8(39).1.37-47
3. Tulupov, V., Onyshchuk, S. (2021). Research of surface reinforcement technologies for machine details. Technical Sciences and Technologies, 3 (25), 55–60. https://doi.org/10.25140/2411-5363-2021-3(25)-55-60
4. Posuvailo, V., Shovkoplias, M., Romaniv, M., Malinin, V. (2021). Comparison of methods of surface strengthening of machine parts by coatings . Bulletin of Cherkasy State Technological University, 26 (4), 83–97. https://doi.org/10.24025/2306-4412.4.2021.253298

5. Maksymuk, O. V. (2020). The peculiarities in contact interaction and wear of thin-walled elements of construction. Matematychni Metody Ta Fizyko-Mekhanichni Polya, 63 (1). https://doi.org/10.15407/mmpmf2020.63.1.133-148
6. Slavov, S. D., Dimitrov, D. M., Mincheva, D. Y., Dzyura, V., Maruschak, P., Semehen, V. (2025). Microstructure and Microhardness Research of Steel 304 After Forming Partially Regular Reliefs by Ball Burnishing Operation. Materials, 18 (7), 1565. https://doi.org/10.3390/ma18071565
7. Zhang, L., Wu, Z. (2023). A mini-review of surface severe plastic deformation methods and their effects on steel and stainless steel. Proceedings of the Institution of Mechanical Engineers, Part L: Journal of Materials: Design and Applications, 238 (3), 397–415. https://doi.org/10.1177/14644207231190491
8. Cao, S. C., Zhang, X., Lu, J., Wang, Y., Shi, S.-Q., Ritchie, R. O. (2019). Predicting surface deformation during mechanical attrition of metallic alloys. Npj Computational Materials, 5 (1). https://doi.org/10.1038/s41524-019-0171-6
9. Wang, G., Tong, Y., Liang, L., Zhang, M., Zhao, M., Li, L. (2025). Indentation deformation mechanism of combined-strengthened modified layer in low-alloy steel under the influence of hydrogen. Corrosion Science, 242, 112579. https://doi.org/10.1016/j.corsci.2024.112579
10. Luo, Q., Kitchen, M. (2023). Microhardness, Indentation Size Effect and Real Hardness of Plastically Deformed Austenitic Hadfield Steel. Materials, 16 (3), 1117. https://doi.org/10.3390/ma16031117
11. Shen, Z., Su, Y., Liang, Z., Long, X. (2024). Review of indentation size effect in crystalline materials: Progress, challenges and opportunities. Journal of Materials Research and Technology, 31, 117–132. https://doi.org/10.1016/j.jmrt.2024.06.071
12. Shul'zhenko, A. A., Jaworska, L., Sokolov, A. N., Romanko, L. A., Gargin, V. G., Belyavina, N. N. et al. (2018). Structure and Electrophysical Properties of the Diamond-Graphen-Silicon Carbide Composite. Journal of Superhard Materials, 40 (6), 435–438. https://doi.org/10.3103/s1063457618060102
13. Skripchenko, N., Tkachuk, M., Nedilko, K., Kyrychuk, D, Borysenko, S., Kasai, O. (2016). Contact interaction of complex-shaped details with local compliance of the surface layer. Bulletin of NTU "KhPI". Series: Engineering and CAD, 39 (1211), 93–101. Available at: https://repository.kpi.kharkov.ua/server/api/core/bitstreams/a6ff27d4-67bc-4980-a387-bce9abed66e6/content
14. Properties and Selection: Irons, Steels, and High-Performance Alloys (1990). ASM Handbook. https://doi.org/10.31399/asm.hb.v01.9781627081610
15. AISI 347 Stainless Steel Datasheet. Ferrobend.
16. Schober, P., Boer, C., Schwarte, L. A. (2018). Correlation Coefficients: Appropriate Use and Interpretation. Anesthesia & Analgesia, 126 (5), 1763–1768. https://doi.org/10.1213/ane.0000000000002864